PHYSICAL REVIEW C **81**, 044305 (2010)

Nuclear spectroscopy above isomers in $^{148}_{67}Ho_{81}$ and $^{149}_{67}Ho_{82}$ nuclei: Search for core-excited states in ^{149}Ho

J. Kownacki,[1,*] Ch. Droste,[2] T. Morek,[2] E. Ruchowska,[3] M. Kisieliński,[1,3] M. Kowalczyk,[1,2] R. M. Lieder,[4] J. Perkowski,[5] J. Andrzejewski,[5] P. J. Napiorkowski,[1] K. Wrzosek-Lipska,[1,2] M. Zielińska,[1] A. Kordyasz,[1] A. Korman,[3] W. Czarnacki,[3] K. Hadyńska-Klęk,[1,2] E. Grodner,[2] J. Srebrny,[1] J. Mierzejewski,[1,2] and A. Król[5]

[1]*Heavy Ion Laboratory, University of Warsaw, Warsaw, Poland*

[2]*Nuclear Physics Division, Institute of Experimental Physics, University of Warsaw, Warsaw, Poland*

[3]*The Andrzej Sołtan Institute for Nuclear Studies, Świerk, Poland*

[4]*Institut für Kernphysik Forschungszentrum Jülich, Jülich, Germany*

[5]*Faculty of Physics, University of Łódź, Łódź, Poland*

(Received 7 December 2009; published 7 April 2010)

The excited states of ^{148}Ho and ^{149}Ho isotopes are studied using γ-ray and electron spectroscopy in off-beam and in-beam modes following ^{112,114}Sn(^{40}Ar, $xnyp$) reactions. Experiments include measurements of single γ-rays and conversion electron spectra as well as γ-γ, electron-γ, γ-t, and γ-γ-t coincidences with the use of the OSIRIS-II 12-HPGe array and conversion electron spectrometer. Based on the present results, the level schemes of ^{148}Ho and ^{149}Ho are revised and significantly extended, up to about 4 and 5 MeV of excitation energy, respectively. Spin and parity of 5^- are assigned to the 9.59-s isomer in ^{148}Ho based on conversion electron results. Previously unobserved γ rays feeding the 10^+ isomer in ^{148}Ho and the $27/2^-$ isomer in ^{149}Ho nuclei are proposed. Shell-model calculations are performed. Possible core-excited states in ^{149}Ho are discussed.

DOI: 10.1103/PhysRevC.81.044305 PACS number(s): 27.60.+j, 23.20.−g, 21.60.Cs

I. INTRODUCTION

The mass region of $A \sim 150$ was investigated using the ^{40}Ar + ^{112,114}Sn reactions at an energy of about 5 MeV/nucleon, in an attempt to study the isomers as well as level structures of nuclei in the vicinity of the $N = 82$-neutron closed shell. Nuclei from this region placed beyond the stability line have been the subject of a few investigations, for example, Refs. [1–6]. However, when this work was started, there was no information available on the high-spin levels of the ^{148}Ho and ^{149}Ho isotopes above the 10^+ [2,3] and $27/2^-$ [6] isomers, respectively.

The nucleus $^{148}_{67}Ho_{81}$ has three valence protons and one neutron hole with respect to the ^{146}Gd core nucleus. This nucleus can reach high spins within the valence nucleon space; an extremely high-spin state with $J^\pi = 16^-$ could be, for example, of $\pi(h^3_{11/2})\nu d^{-1}_{5/2}$ configuration, so that core-excited states would probably not appear. On the contrary, there should be competition between proton excitations, corresponding to the proton excited states in ^{148}Ho, and proton-neutron-hole excitations observed in ^{146}Tb, where states with about the same spin occur at about the same energy.

The nucleus $^{149}_{67}Ho_{82}$ has three valence protons with respect to the ^{146}Gd core nucleus. One of the motivations of the present work was to search for particle-hole excitations that are present in ^{146}Gd and should also appear above the $(27/2^-)$ isomeric state in ^{149}Ho.

II. EXPERIMENT

The $^{40}Ar^{8+}$ pulsed beam, used to populate the ^{148}Ho and ^{149}Ho nuclei via the ^{112,114}Sn(^{40}Ar,$xnyp$) reaction, was provided by the HIL (Heavy Ion Laboratory, University of Warsaw) cyclotron. The γ-γ and e-γ coincidences in the in-beam and off-beam modes have been studied. The self-supporting targets were prepared from metallic ^{112}Sn and ^{114}Sn, enriched to 92% and 86%, respectively. The OSIRIS-II array, consisting of 12 Compton-suppressed HPGe detectors (2 detectors at 25°/155°, 4 detectors at 38°/142°, 4 detectors at 63°/117°, and 2 detectors at 90° with respect to the beam direction), has been used in the reported experiments in different configurations (e.g., 11 HPGe detectors were assembled, together with an electron spectrometer chamber; see Table I for some details of the experiments). Internal conversion electron spectra in coincidence with γ rays have been measured. Out-of-beam measurements of conversion electrons were performed to unambiguously deduce multipolarity assignments for specific transitions in the decay path of the 10^+ isomer observed [2] in the ^{148}Ho nucleus. Electrons were detected with six cooled (with three Peltier modules) Si(Li) detectors located inside the chamber, in which the combination of two magnetic fields was generated to separate e^+ from e^- and then to transport electrons from the target area to the detectors [7]. Sources of ^{133}Ba and ^{152}Eu were used to calibrate the electron and γ-ray detectors for energies and efficiencies. The transmission curve of the electron spectrometer measured for the magnet configuration used is discussed in a separate publication [7]. Taking advantage of the unique beam pulse structure of the HIL cyclotron, one can measure the γ-γ coincidence spectra in in-beam (2- to 4-ms) and off-beam (4- to 8-ms) modes. Figure 1 displays an example of spectra measured at the begining and at the end of

*jko@slcj.uw.edu.pl

TABLE I. Details of the experiments.

Reaction; type of experiment	Conditions: detectors, beam	Beam energy (MeV)	Target (mg/cm^2)
$^{40}Ar^{8+} + ^{112}Sn$	HPGe's, e^- spectrometer	232	8
γ long time	10 μs = 1 channel	206	
$\gamma\gamma$ time	2 ms on/4 ms off 4 ms on/8 ms off Ge-Ge, Ge-t_{RF}		
Electron-γ	2 ms on/4 ms off	200	4.5
$^{40}Ar^{8+} + ^{114}Sn$	HPGe's, e^- spectrometer	206	6.5
γ long time	10 μs = 1 channel		
$\gamma\gamma$-time	2 ms on/4 ms off 4 ms on/8 ms off Ge-Ge, Ge-t_{RF}		
Electron-γ	2 ms on/4 ms off	200	4.0

the beam-off period, showing the existence of isomers in the time region of milliseconds and several microseconds.

Angular distribution (anisotropy) R_{AD} ratios were deduced from OSIRIS-II data to get an indication of the multipolarities of the observed γ transitions. Spectra used for determination of R_{AD} values were obtained from matrices containing the coincidences between one detector at a specific angle and all the other HPGe detectors. Gating the matrices on the axes containing information from all detectors and taking into account the efficiencies of the different detectors, one can determine angular distribution ratios $W(25°)/W(90°)$, where $W\theta)$ is the intensity of γ rays registered by the detectors placed at angle θ with respect to the beam axis. The coincident spectra for similar angles were summed to obtain a higher statistical accuracy for the R_{AD} ratios.

III. RESULTS

A. The ^{148}Ho nucleus

The ^{148}Ho nucleus, with 67 protons and 81 neutrons, has been studied in fusion evaporation reactions and discussed in terms of the spherical shell model [2,3]. In the present study an attempt was made to establish experimentally the γ rays that are feeding the 10^+ isomer in ^{148}Ho, which was previously reported by Broda *et al.* [2].

Ten of the prompt γ rays observed in the studied reactions were assigned to ^{148}Ho as feeding the 10^+ isomer, that is, the 150-, 155-, 183-, 283-, 295-, 339-, 426-, 544-, 545-, and 952-keV lines (Fig. 2). The assignments are based on X-γ relations and prompt-delayed γ-γ coincidences. Especially X-γ coincidences were very helpful in identification of the observed transitions. Each of the γ lines just listed is in coincidence with the K_α and K_β Ho X rays and they are assigned to the ^{148}Ho nucleus, as they are not observed in the in-beam coincidences performed for ^{149}Ho and were not seen in the available data concerning other Ho isotopes that could be produced in reactions used.

Another piece of information comes from the spectra measured taking advantage of natural high-frequency beam bunching of the HIL cyclotron. It is based on coincidences between γ rays emitted in the prompt time range, that is, during the beam micropulses with those emitted between them. (The separation of two beam micropulses is given

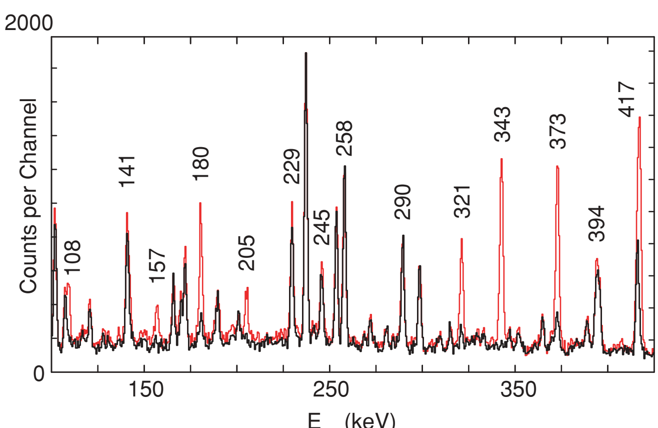

FIG. 1. (Color online) Example of two γ-ray spectra collected for a time of 300 μs at the beginning (red line) and at the end (black line), 5.8 ms later, of the beam-off period, respectively. One can see delayed γ rays with energies of 141, 157, 205, 343, and 417 keV ($T_{1/2}$ = 1.23 ms), which belong to the ^{146}Tb nucleus, and 108, 180, 321, and 373 keV ($T_{1/2}$ = 2.62 ms), which belong to ^{148}Ho. The 141-keV line appears in both spectra because, apart from the 141-keV line in ^{148}Ho, there is also a 138-keV γ ray in ^{146}Tb and, additionally, a 140-keV line in ^{147}Gd (radioactive decay). For the 417-keV γ ray there is an admixture of the 416.5-keV isomeric (150-ms) transition from the ^{146}Dy nucleus.

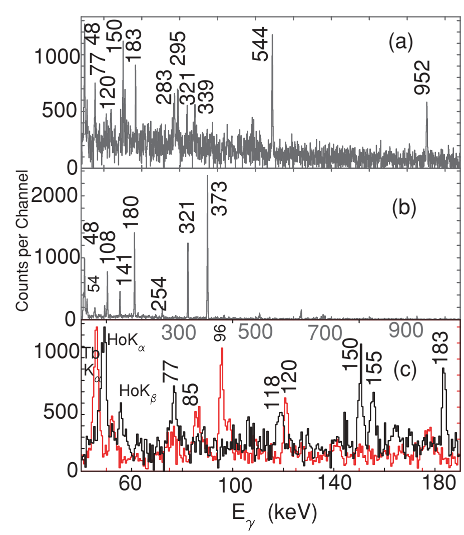

FIG. 2. (Color online) γ rays (a) feeding and (b) de-exciting the 10^+, 2.62-ms isomer in ^{148}Ho obtained by gating on the strongest transitions above and below the isomeric state, respectively. (c) Low-energy X-γ coincidence spectrum showing X rays obtained by summing spectra gated on γ rays feeding the 10^+ isomer in ^{148}Ho (black line). A similar sum spectrum obtained by gating on γ rays feeding the 10^+ isomer in ^{146}Tb (red line) is shown for comparison.

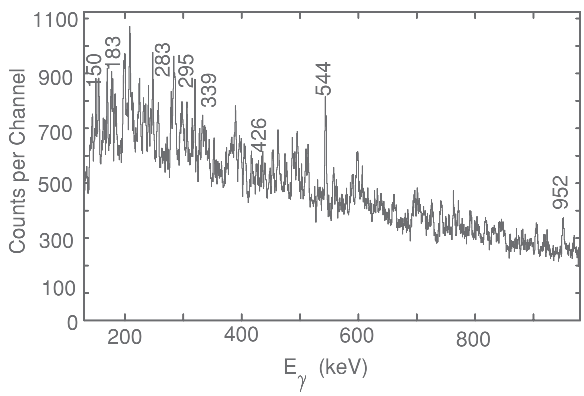

FIG. 3. Prompt-delayed γ-γ coincidence spectrum obtained by gating on the 373-keV isomeric $10^+ \to 7^-$ transition in ^{148}Ho registered between the beam micropulses of the cyclotron while the prompt γ-ray is emitted during the beam micropulses. Lines marked with energy values belong to the newly proposed cascade placed above the 10^+ isomer.

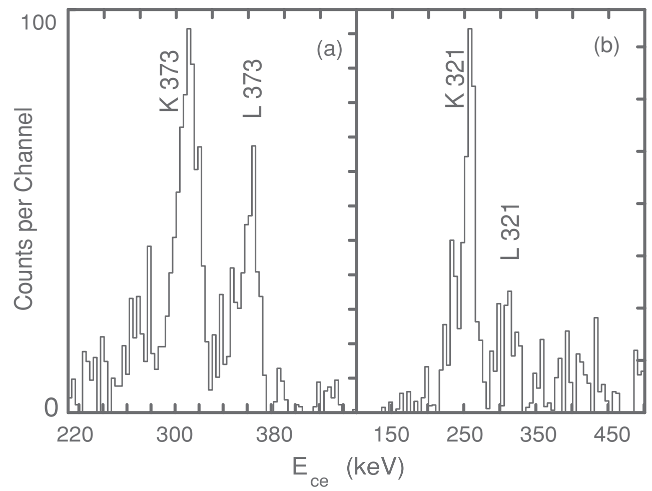

FIG. 4. (a) Off-beam background-corrected e^- spectrum gated on the 180- and 321-keV γ rays in ^{148}Ho. (b) Off-beam background-corrected e^- spectrum gated on the 373-keV γ ray in ^{148}Ho.

by the period $T = 1/f$. For ^{40}Ar^{+8} the frequency is $f =$ 12.51 MHz and $T = 79.94$ ns.) Prompt-delayed coincident spectra that were created in this way include coincident prompt γ lines preceding (feeding) the isomers. In Fig. 3 an example of such a prompt-delayed spectrum obtained in the ^{112,114}Sn(^{40}Ar,$xnyp$) reactions is shown. This spectrum, with a gate set on the delayed 373-keV γ line, clearly shows the association of the proposed γ lines with the ^{148}Ho nucleus.

Electron spectra for the 373-keV line, gated on the 180- and 321-keV γ rays, and for the 321-keV line, gated on the 373-keV γ ray, in ^{148}Ho measured in the off-beam mode are shown in Fig. 4.

From the conversion coefficients α_K and $\alpha_{L+M+\cdots}$ and the $K/(L+M+\cdots)$ ratios given in Table II, it was concluded that the 373-keV transition in ^{148}Ho is of an E3 character—in agreement with the former [2,3] assumption based on the $\alpha_{\rm tot}$ value estimated from the intensity balance. Figure 5, showing the α_K values obtained for several transitions, demonstrates agreement of our electron conversion results with theoretical predictions. In addition to results for transitions in ^{148}Ho (E2, 321 keV; and E3, 373 keV), α_K values of the well-known transitions in the ^{145,147,149}Eu [9,10] isotopes, in ^{146}Dy [11], and in ^{149}Dy [12] are shown. The α_K values of the 343-keV E2 and 417-keV E3 transitions in ^{146}Tb were measured for the first time.

The level scheme based on the data obtained in the ^{112,114}Sn(^{40}Ar, $xnyp$) reactions is shown in Fig. 6, where the new bandlike structure above the 10^+ isomer is also given. Formerly [13], based on the decay characteristics, a spin-parity assignment of (6^-) was proposed for the 9.59-s isomeric state in ^{148}Ho. In Refs. [2] and [3] an M1 nature for the 321-keV transition from the 7^- level to this state was suggested. However, our conversion electron results (Fig. 4 and Table II) firmly indicate an E2 nature for this transition. Based on these results, spin and parity of 5^- can be assigned to the $0 + x$-keV, 9.59-s isomer. Spin and parity of 6^- cannot be excluded when considering the β^+/EC data [13–16] for ^{148}Ho (the 9.59-s isomeric state) $\to^{148}$Dy decay. The $I^\pi = 6^-$ as well as the $I^\pi = 5^-$ assignments would rather contradict direct feeding of the 8^+, 2834-keV state in ^{148}Dy with $\log ft = 6.97$ ($I_{{\rm EC}+\beta^+} = 0.35$) or $\log ft = 6.52$ if ($I_{{\rm EC}+\beta^+} = 1.0$ [16]), suggesting the first forbidden Gamow-Teller decay with $\Delta I = 0, 1$ and $\Delta\pi =$ yes. Otherwise one

TABLE II. Properties of the conversion electron lines assigned to $^{148}_{67}$Ho$_{81}$: γ-ray energies E_γ, conversion electron energies $E_{\rm EC}$, experimental and theoretical $K/L+M+\cdots$ ratios, and absolute conversion coefficients α_K and $\alpha_{L+M+\cdots}$.

E_γ (keV)	$E_{\rm EC}$ (keV)	Shell	$K/L+M+\cdots$ ratio[a], $\alpha_{\rm exp}$[a]	Theory[b]				Multipolarity
				E1	E2	M1	M3	
321		$K/(L+M+\cdots)$	3.1(7)	7.030	**3.151**	5.800	1.330	E2
	265.4	α_K	0.043(8)	0.013	**0.041**	0.087	0.121	E2
		$\alpha_{L+M+\cdots}$	0.013(5)	0.002	**0.013**	0.015	0.091	E2
73		$K/(L+M+\cdots)$	1.8(5)	7.090	4.340	6.920	**1.689**	E3
	317.4	α_K	0.065(10)	0.009	0.027	0.058	**0.076**	E3
		$\alpha_{L+M+\cdots}$	0.046(8)	0.001	0.008	0.010	**0.045**	E3

[a]From the present experiment.
[b]From Ref. [8].

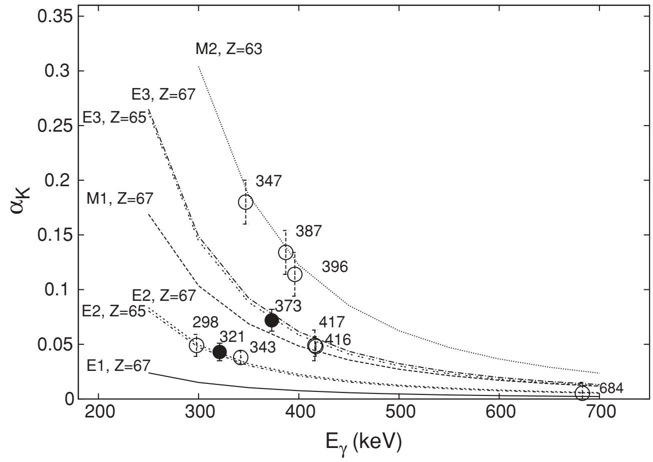

FIG. 5. The α_K conversion coefficients measured in the off-beam mode using the reaction ^{40}Ar + ^{112}Sn for ^{148}Ho (E2, 321 keV, and E3, 373 keV; shown by filled ovals), ^{146}Tb (E2, 343 keV, and E3, 417 keV), ^{149}Eu (M2, 347 keV), ^{147}Eu (M2, 396 keV), ^{145}Eu (M2, 387 keV), and ^{149}Dy (E2, 298 keV) as well as ^{146}Dy (E3, 416 keV, and E2, 684 keV).

would expect a log ft value of at least about 8.5 (first forbidden unique transition, $\Delta I = 2$, $\Delta\pi$ = yes) for the Gamow-Teller decay to this state. Nevertheless, there is a possibility that the 2834-keV level is indirectly fed by unobserved weak γ transitions.

The 10^+, 2.62-ms isomer is suggested [2,3] to be of $[\pi h_{11/2} \nu h_{11/2}^{-1}]$ configuration, whereas the 9.59-s, long-lived isomer [3,15,16] is probably of $[\pi h_{11/2} \nu s_{1/2}^{-1}]$ nature. The 10^+ isomer decays via E3 transition to $[\pi h_{11/2} \nu d_{5/2}^{-1}]7^-$ state, and consequently the 321-keV transition has to proceed via $\nu d_{5/2}^{-1} \rightarrow \nu s_{1/2}^{-1}$ configurations to the 5^- state.

Finally, the 180-, 141-, and 108-keV transitions remain of M1 character as was assumed in Ref. [3]. The intensity balance of the postisomeric transitions in ^{148}Ho does not contradict an E2 nature of the 321-keV transition because the difference between ingoing and out-going intensities for the 321-keV, 7^- level does not exceed 3%.

One has to consider the problem of nonexistence of the crossover $7^- \rightarrow 5_2^-$ 288-keV transition, which could compete with the 180-keV, M1 and 321-keV, E2 transitions. We did not find the 288-keV line: the upper limit for its intensity is $\leqslant 0.74$, compared to $I_\gamma = 100$ for the 321-keV line.

According to the Weisskopf estimation the 180-keV transition is about 3 orders of magnitude faster than the 288-keV transition would be. From the other side the 321-keV, E2 transition should be slightly faster than the 288-keV, E2 transition, owing to the energy factor.

The explanation of the E2, 321-keV transition strengths compared to the M1, 180-keV transition probably underlies the structure of the initial and final levels involved, making the E2, 321-keV transition allowed and the M1, 180-keV one hindered.

The information on new transitions assigned to the ^{148}Ho nucleus is summarized in Table III. The 951.8-keV transition is supposed to be of M1 + E2 nature, so the 1646-keV level can be of spin 11 and positive parity. If the 545-keV transition (or 544-keV transition) is of E1 character,

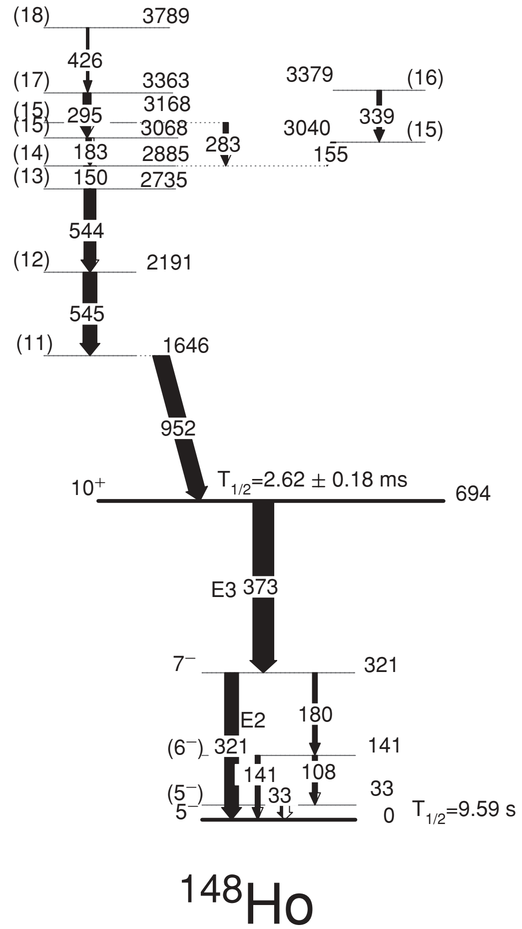

FIG. 6. Partial level scheme of ^{148}Ho resulting from the present work. Levels placed above the 10^+ isomer are newly assigned. As the connection of this level scheme to the 1^+ ground state of ^{148}Ho is unknown, a value of x keV must be added to the energy of each level.

then all higher-lying states would be of negative parity, which is supported by the present shell model calculation (see Sec. IV).

In the present study half-life information was obtained by examining background-subtracted time spectra deduced from the γ-time matrices. In these spectra the number of emitted γ rays was plotted versus time measured with respect to beam macropulses and was fitted to an exponential decay curve. The time spectra of the 373-, 321-, 180-, and 108-keV transitions are shown in Figs. 7–10. A half-life of 2.62 ± 0.18 ms for the 10^+ level was obtained as a weighted average of the half-life values for the 373-, 321-, and 180-keV lines. This value is in reasonable agreement with the value deduced by Broda *et al.* [2,3], *viz.*, $T_{1/2} = 2.35 \pm 0.04$ ms. The half-life obtained from the analysis of the 108-keV γ transition was not taken into account, as this line seems to be contaminated.

B. The ^{149}Ho nucleus. Feeding of the ($27/2^-$), 59-ns isomeric state

The γ-γ coincidence spectra in the in-beam mode for ^{149}Ho are shown in Fig. 11. The sum spectrum with the in-beam

TABLE III. Summary of γ rays observed in ^{148}Ho above the 10^+ isomer following the ^{112}Sn(^{40}Ar, $p3n$) reaction at 206 MeV.

E_γ (keV)	I_γ^{rel}	$R_{AD} = \frac{W(25^\circ)}{W(90^\circ)}$ [a]	Multipolarity	$I_i^\pi \rightarrow I_f^\pi$
150.0	100 ± 10	0.7	D[c]	(14) → (13)
154.8	90.4 ± 9.2			(15) → (14)
182.9	82.0 ± 8.4	1.0	M1 + E2	(15) → (14)
283.2	33.9 ± 4.1	1.0	M1 + E2	(15) → (14)
295.2	74.0 ± 7.6	1.6	E2	(17) → (15)
339.3	68.2 ± 7.1			(16) → (15)
426.0	33.5 ± 3.9			(18) → (17)
545[b]	296 ± 30	0.8	D	$\Delta I = 1$
951.8	123 ± 13	1.2	D, Q[c]	$(11^+) \rightarrow (10^+)$

[a]The $W(25^\circ)/W(90^\circ)$ ratio was used because the anisotropy at these angles is most pronounced. W(θ) is the intensity of γ rays registered by detectors placed at angle θ with respect to the beam axis. The expected R_{AD} value for the E2 transition is 1.4, whereas the R_{AD} for pure M1 is 0.8. Mean error of R_{AD} does not exceed 15%.
[b]Double line composed of 544.3- and 545.2-keV transitions.
[c]D, dipole; Q, quadrupole.

gates on the 1180-, 1082-, 792-, 685-, 531-, and 435-keV transitions above the $(27/2^-)$, 59-ns isomer, compared to the sum spectrum with the gates on the 1560-, 726-, 306-, and 144-keV γ-rays placed below the isomer, is displayed, providing evidence for the mutual correspondence of both sequences of γ rays. The $(27/2^-)$, 59-ns isomer [6] decays via a $\Delta I = 2$ cascade consisting of the 1560-, 726-, 306-, and 144-keV γ rays built on the $(11/2^-)$ ground-state level. Another cascade de-excites the 2591-keV, $(23/2^-)$ level via the 185-, 383-, 644-, and 1379-keV transitions. This sequence was described by Wilson *et al.* [6] as a cascade of E1 (185-keV line) and E2 transitions (383- and 644-keV lines), while the 1379-keV transition was assumed to be of M2 character. Our shell model calculation concerning this sequence is consistent with an E2 assignment [6] for both the 383- and the 644-keV transitions. The lifetime of the $(15/2^+)$ level is still unknown and a separate measurement would be necessary to confirm the structure of this band.

The γ rays feeding the 59-ns isomer were observed within a 200-ns time gate measured in the in-beam mode. An analysis of the prompt-delayed coincidence spectra in ^{149}Ho was also performed. In Fig. 12 the coincidence spectra gated by the delayed 144-keV and prompt 1180-keV γ rays are shown, illustrating, additionally, relations between the lines feeding and those de-exciting the 59-ns isomer. The transitions feeding the 59-ns isomer in ^{149}Ho were extracted by setting a time gate before (and after) the prompt time peak of the E_γ-E_γ-t events, of the selected γ-ray transitions. A comparison of the two spectra (Fig. 13) with gates set on the 792-keV line (above the isomer) and the 726-keV line (below the isomer) shows the γ-rays de-exciting and feeding the $(27/2^-)$ isomeric state, respectively.

Above the $(27/2^-)$ isomeric state a new 113-keV transition, most probably of M1 character, is proposed. Three newly introduced bands are (a) a sequence of the 1180-, 792-, and 685-keV transitions, which might connect the states of negative parity; (b) a possible negative-parity sequence consisting of

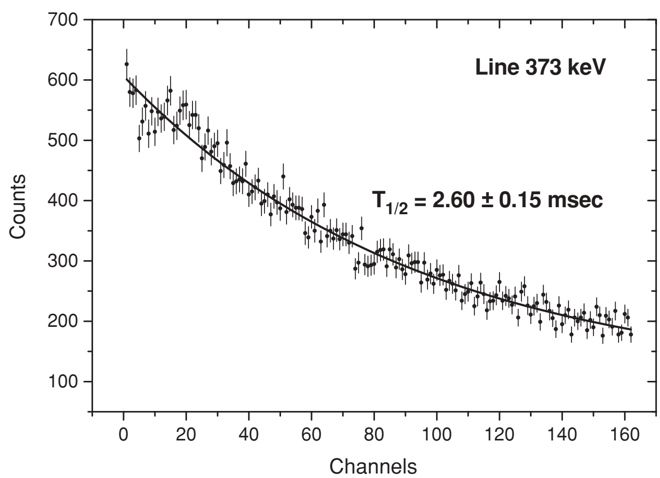

FIG. 7. Time spectrum for the 373-keV γ ray in ^{148}Ho measured in the off-beam period.

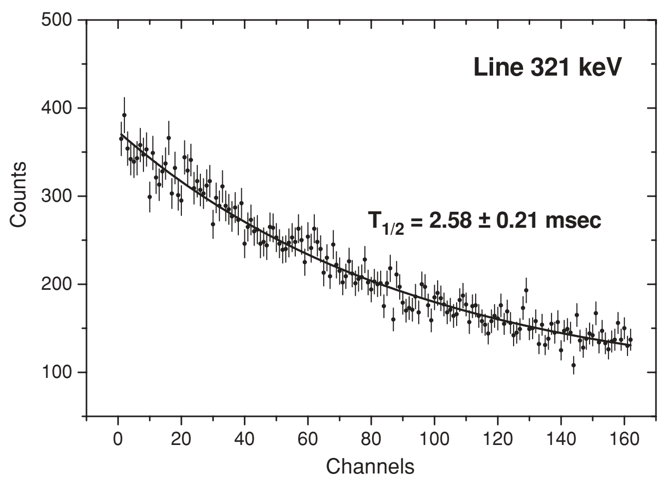

FIG. 8. Time spectrum for the 321-keV γ ray in ^{148}Ho measured in the off-beam period.

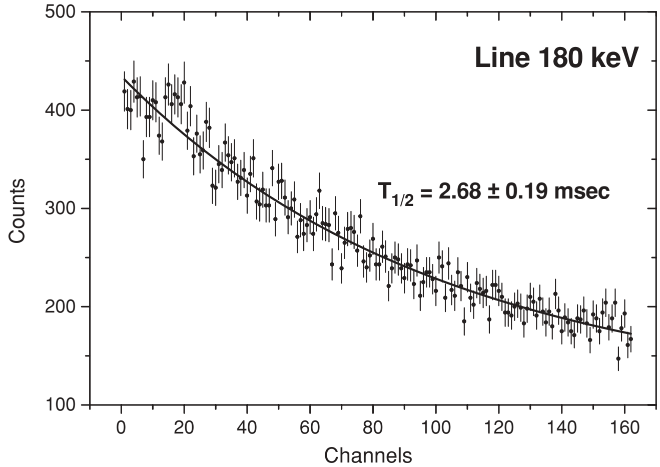

FIG. 9. Time spectrum for the 180-keV γ ray in ^{148}Ho measured in the off-beam period.

two E2 transitions, 1944 and 531 keV; and (c) three transitions, 1082, 399, and 435 keV, forming possible positive-parity band. Properties of the observed transitions belonging to ^{149}Ho are summarized in Table IV and the resulting level scheme is presented in Fig. 14.

IV. CALCULATION OF LEVEL ENERGIES IN THE ^{148}Ho AND ^{149}Ho NUCLEI

A. ^{148}Ho

The ^{148}Ho nucleus can be considered to consist of a ^{146}Gd core, three valence protons, and one neutron hole in the $N = 82$ shell. If the energy of the ^{146}Gd core is set to 0, the total Hamiltonian of the four valence particles neglecting three- and four-body interactions can be written as

$$H = \sum_{i}^{4} H(i) + \sum_{i<j} H(i, j).$$

The Hamiltonians $H(i)$ are the single-particle energies that can be taken from the experimental excitation energies in ^{147}Tb for protons and from those in ^{145}Gd for neutron holes. The effective interaction matrix elements $H(i, j)$ between two particles can be extracted from experimental energies

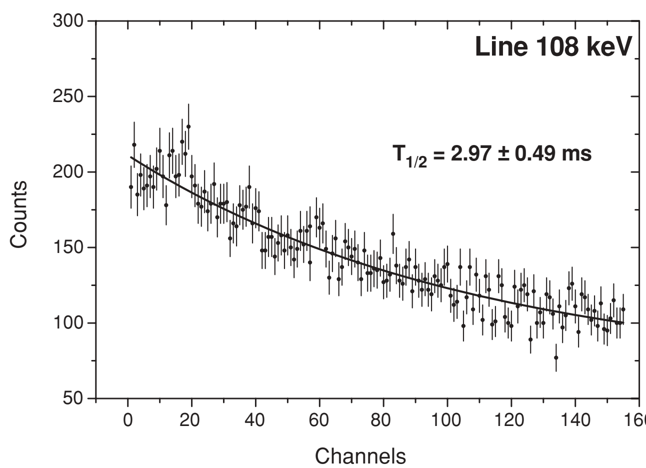

FIG. 10. Time spectrum for the 108-keV γ ray in ^{148}Ho measured in the off-beam period.

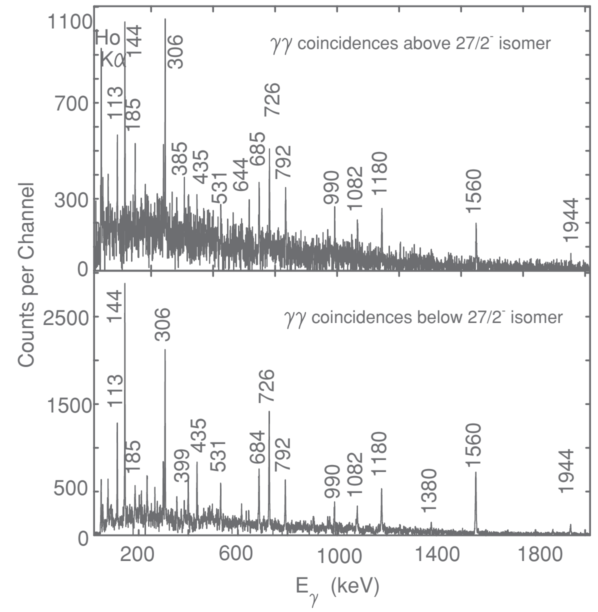

FIG. 11. γ rays de-exciting (bottom) and feeding (top) the $(27/2^-)$, 59-ns isomer in ^{149}Ho. Bottom: sum of in-beam gates on the 1180-, 1082-, 792-, 685-, 531-, and 435-keV γ rays. Top: sum of gates on 1560-, 726-, 306-, and 144-keV γ rays.

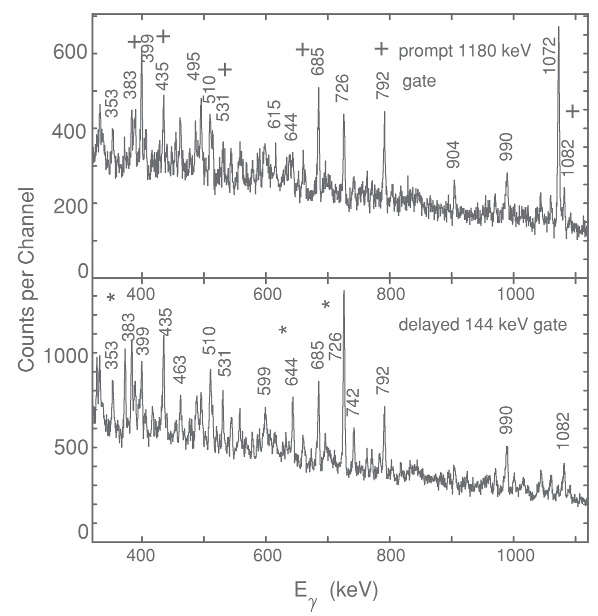

FIG. 12. Part of the prompt-delayed coincidence spectra of ^{149}Ho. Gates were set, respectively, on the 144-keV isomeric $(27/2^-) \rightarrow (23/2^-)$ transition (bottom) and on the 1180-keV prompt transition feeding the $(27/2^-)$ isomeric state (top) in ^{149}Ho. Lines marked with asterisks belong to the cascade placed below the $(27/2^-)$ isomeric state; lines marked with plus signs are the cascades feeding the isomer.

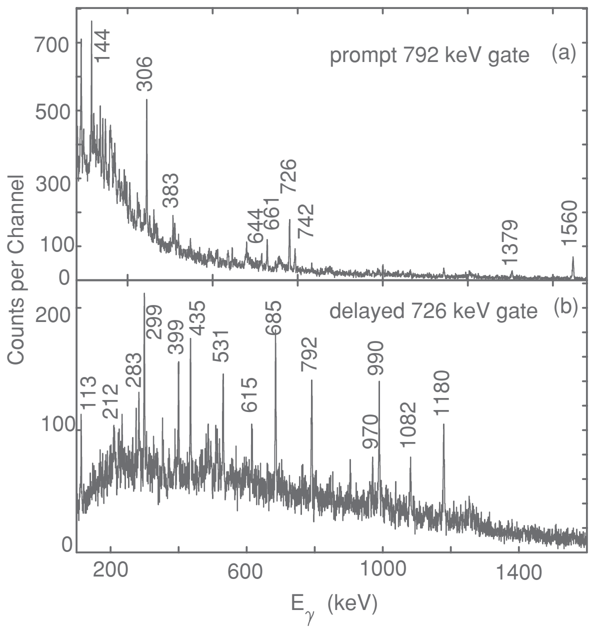

FIG. 13. Prompt-delayed coincidence spectra. The gate was set on (a) the 792-keV prompt transition and on (b) the 726-keV delayed transition de-exciting the $(19/2^-)$ state placed below the $(27/2^-)$ isomeric state in ^{149}Ho. Lines in (a) denote cascades placed below the $(27/2^-)$ isomeric state.

in nuclei consisting of a ^{146}Gd core plus two particles, in this case ^{148}Dy and ^{146}Tb. Experience (in the mass region of $A \sim 208$ [17]) has shown that it is enough to truncate the configuration space to levels within the main shells and include, in our case, only the orbitals $1h_{11/2}$, $2d_{3/2}$, and $3s_{1/2}$ for protons and $2d^{-1}_{3/2}$, $3s^{-1}_{1/2}$, $1h^{-1}_{11/2}$, $1g^{-1}_{7/2}$, and $2d^{-1}_{5/2}$ for neutron holes. The calculation difficulties are partially avoided by using the experimental energies of levels built of three (^{149}Ho and ^{147}Dy), two (^{148}Dy and ^{146}Tb), and one (^{147}Tb and ^{145}Gd) valence particles. The total Hamiltonian of ^{148}Ho can be written as

$$\begin{aligned} H[\pi(123)\nu(4)] &= H[\pi(1,2,3)] + H[\pi(1,2)\nu(4)] \\ &\quad + H[\pi(2,3)\nu(4)] + H[\pi(3,1)\nu(4)] \\ &\quad - H[\pi(1,2)] - H[\pi(2,3)] - H[\pi(3,1)] \\ &\quad - H[\pi(1)\nu(4)] - H[\pi(2)\nu(4)] - H[\pi(3)\nu(4)] \\ &\quad + H[\pi(1)] + H[\pi(2)] + H[\pi(3)] + H[\pi(4)], \end{aligned}$$

where the numbers 1–3 stand for three protons outside the closed shell $Z = 64$, and the number 4 is associated with one neutron hole in an $N = 82$ closed shell.

The double counting of the two-particle interactions in the three-particle terms is corrected by subtraction of the two-particle terms. The excitation energies related to nuclear masses can be obtained [18] as

$$\begin{aligned} E(^{148}\text{Ho}) &= E(^{149}\text{Ho}) + 3E(^{147}\text{Dy}) - 3E(^{148}\text{Dy}) \\ &\quad - 3E(^{146}\text{Tb}) + 3E(^{147}\text{Tb}) + E(^{145}\text{Gd}) + E_0, \end{aligned}$$

where

$$\begin{aligned} E_0 &= -M(^{148}\text{Ho}) + M(^{149}\text{Ho}) + 3M(^{147}\text{Dy}) \\ &\quad - 3M(^{148}\text{Dy}) - 3M(^{146}\text{Tb}) + 3M(^{147}\text{Tb}) \\ &\quad + M(^{145}\text{Gd}) - M(^{146}\text{Gd}). \end{aligned}$$

As a result, we obtain from the calculation the energy of 1688 keV for the 11^- state with the $\pi(h^3_{11/2})_{27/2}\nu d^{-1}_{5/2}$ configuration. Calculations were performed using experimental excitation energies in ^{149}Ho, ^{147}Dy, ^{148}Dy, ^{146}Tb, ^{147}Tb,

TABLE IV. Summary of the γ-ray data observed in ^{149}Ho following the ^{112}Sn(^{40}Ar,$p2n$) reaction at a beam energy of 206 MeV.

E_γ (keV)	$I^{\rm rel}_\gamma$	$R_{\rm AD} = \frac{W(25^\circ)}{W(90^\circ)}$ [a]	Multipolarity	$I^\pi_i \to I^\pi_f$
113.2	35.6 ± 3.6	Isotropic		$(31/2, 29/2) \to (27/2^-)$
143.8	62.4 ± 6.4	Isotropic		$(27/2^-) \to (23/2^-)$
185.0	18.3 ± 4.4	Isotropic		$(23/2^-) \to (23/2^+)$
306.0	64.9 ± 6.6	Isotropic		$(23/2^-) \to (19/2^-)$
383.1	25.2 ± 4.9	Isotropic		$(23/2^+) \to (19/2^+)$
399.4	16.2 ± 1.7	1.30	E2	$(35/2, 37/2) \to (31/2, 33/2)$
434.7	26.9 ± 2.7	1.20	E2	$(39/2, 41/2) \to (35/2, 37/2)$
530.6	24.2 ± 2.5	1.45	E2	$(35/2^-) \to (31/2^-)$
644.3	30.1 ± 4.5	Isotropic		$(19/2^+) \to (15/2^+)$
685.0	47.5 ± 4.8	0.85	D[b]	$(39/2, 41/2) \to (37/2, 39/2)$
725.8	100 ± 10	Isotropic		$(19/2^-) \to (15/2^-)$
791.7	45.2 ± 4.6	1.45	E2	$(37/2, 39/2) \to (33/2, 35/2)$
1082.0	39.1 ± 4.1	0.80	D[b]	$(31/2, 33/2) \to (29/2, 31/2)$
1180.0	67.2 ± 7.3	1.16	E2	$(33/2, 35/2) \to (29/2, 31/2)$
1379.1	42.5 ± 4.4	Isotropic		$(15/2^+) \to (11/2^-)$
1559.8	109 ± 11	Isotropic		$(15/2^-) \to (11/2^-)$
1944.3	37.6 ± 4.0	1.45	E2	$(31/2^-) \to (27/2^-)$

[a]Mean error of $R_{\rm AD}$ does not exceed 15%.
[b]D, dipole.

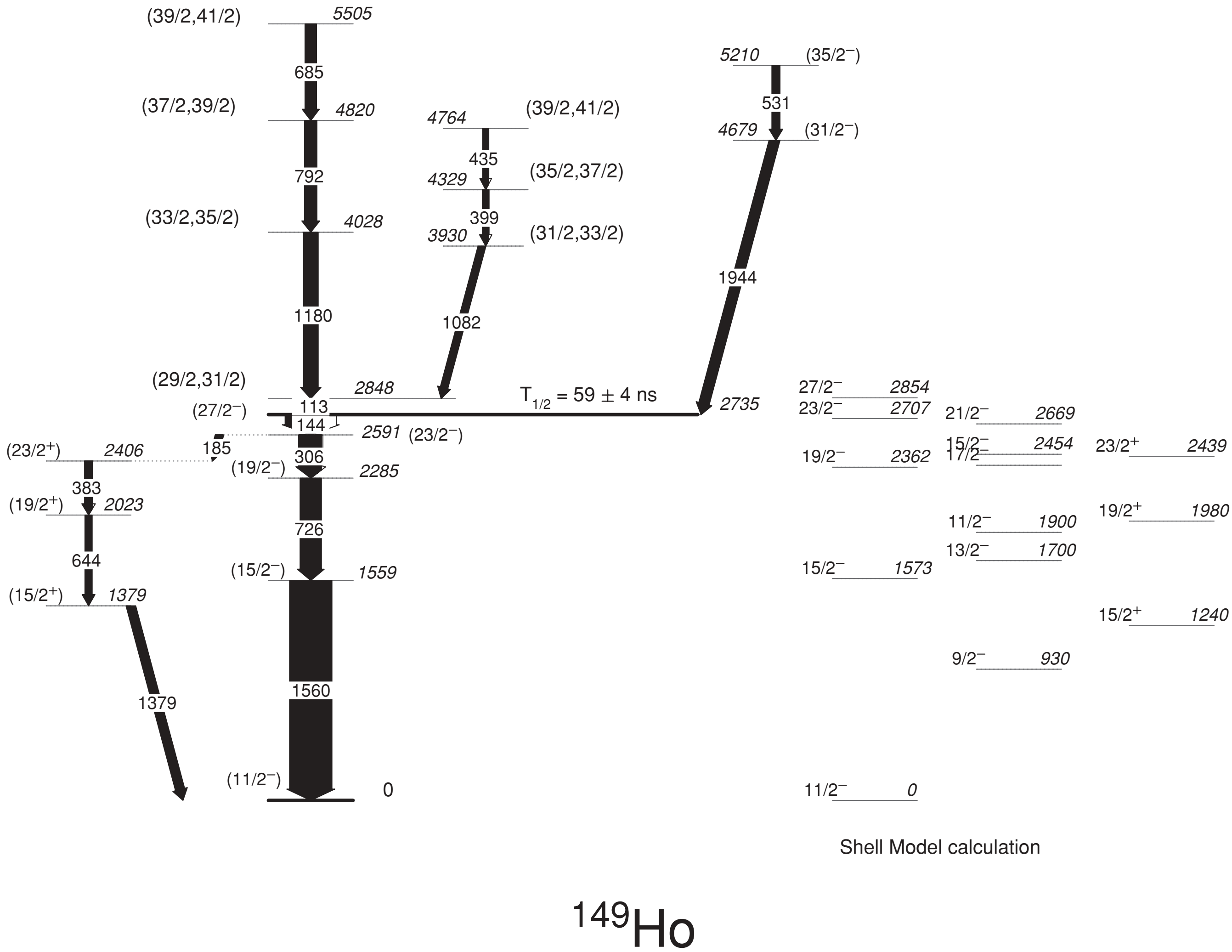

FIG. 14. Partial level scheme for ^{149}Ho extracted from the present work. The levels placed above the $(27/2^-)$ isomer are proposed in this work. Shell-model predictions of the excited states in ^{149}Ho are also shown (see also Table VI). Spin-parity assignments of the $(23/2^+) \rightarrow (19/2^+) \rightarrow (15/2^+)$ cascade are consistent with those of Wilson *et al.* [6] and with our shell-model calculations. All energies are kilo–electron volts.

and ^{145}Gd and the estimated energy of the 8^- state in the ^{146}Tb nucleus. They were restricted to those levels in ^{148}Ho that should originate from simple configurations and for which the amplitude of the leading term is expected to be high.

In Table V the experimental and calculated level energies are compared. The calculated high-spin-state energies are tentatively ascribed to experimental ones, as the parity assignments are not known definitively above the (10^+) isomeric state. Also, an additional uncertainty is introduced into the calculation because the $(\pi h_{11/2} \nu d^{-1}_{5/2})_{3^-,4^-,5^-,8^-}$ states in ^{146}Tb are not well known and therefore the corresponding interactions had to be estimated. It must be stressed that if the 1646-keV level in ^{148}Ho is of positive parity ($I^\pi = 11^+$), then this state can be assigned as a member of the $(\pi h_{11/2} \nu h^{-1}_{11/2})$ configuration, similarly as proposed for ^{146}Tb [19].

According to the remark in Sec. I pointing out the competition between proton and proton-neutron hole excitations, when studying high-spin excited states of the ^{148}Ho nucleus it is interesting to note similarities of its level structure with that observed in ^{146}Tb [19,20].

B. ^{149}Ho

The three valence protons in ^{149}Ho (^{146}Gd + 3 protons) provide the opportunity to predict the energies of states using the coefficients of the fractional parentage (cfp) approach assuming an $(h_{11/2})^3$ configuration and applying the experimental two-proton interaction matrix elements of ^{148}Dy. The squares of cfp's give the probability that a given final state is constructed from a specific "parent" configuration—in this case, a two-particle state. Thus, the j^3 energy levels of ^{149}Ho are calculated in terms of the empirically known $(h_{11/2})^2$ levels of ^{148}Dy. In the ^{149}Ho nucleus, a sequence of $\pi(h_{11/2})^3$ states extending up to the $27/2^-$ isomer at 2735 keV was already [6] known. In the considered case, the total residual interactions

TABLE V. Comparison between experimental and calculated energy levels of ^{148}Ho.

Main configuration	J^π	E_{exc} (keV)	E_{th} (keV)	ΔE, $E_{exp} - E_{th}$ (keV)
$\pi h_{11/2} \nu s_{1/2}^{-1}$	5^-	0	0	
$\pi h_{11/2} \nu d_{3/2}^{-1}$	5^-	33		
$\pi h_{11/2} \nu d_{3/2}^{-1}$	6^-	141	155	−14
$\pi h_{11/2} \nu (d_{3/2}^{-1}, d_{5/2}^{-1})$	7^-	321	290	+31
$\pi h_{11/2} \nu h_{11/2}^{-1}$	10^+	694	709	−15
$\pi h_{11/2} \nu h_{11/2}^{-1}$	11^+		1201	
$\pi (h_{11/2}^3) \nu d_{3/2}^{-1}$	(11_1^-)		1688	
$\pi (h_{11/2}^3) \nu d_{5/2}^{-1}$	(11_2^-)		1796	
$\pi (h_{11/2}^3) \nu d_{3/2}^{-1}$	(12^-)	2191	2257	−66
$\pi (h_{11/2}^3) \nu d_{5/2}^{-1}$	(13^-)	2735	2792	−62
$\pi (h_{11/2}^3) \nu d_{5/2}^{-1}$	(14^-)	2885	2946	−61
$\pi (h_{11/2}^3) \nu d_{5/2}^{-1}$	(15_1^-)	3068	3173	−105
$\pi (h_{11/2}^3) \nu d_{5/2}^{-1}$	(15_3^-)	3168	3218	−50

Δ_J can also be presented as linear combinations of two-particle interactions $\Delta_{J_1}(j, j)$ weighted by the square of the proper cfp as

$$\Delta_J = 3\Sigma_{J_1 \text{even}}[j^2(J_1 j J|\}j^3 J]^2 \Delta_{J_1}(j, j),$$

assuming that there is only one antisymmetric state of the j^3 configuration and a certain value of J. The comparison between experimental and calculated level energies in ^{149}Ho is presented in Table VI. States up to spin $(27/2^-)$ have been considered to have a pure $(h_{11/2})^3$ configuration. Such calculations were performed previously by Wilson *et al.* [6] and Lawson [21], and their results are very close to those presented here. The possible configurations for the newly introduced level structure above the $(27/2^-)$, 59-ns isomer are listed in the lower part of Table VI.

When the nucleus is excited to a state where the maximum total angular momentum of the valence nucleons is less than the angular momentum transferred (in the considered reaction), the only way of describing its states is by introducing particle-hole excitations (also called core excitation). These are thus excited states in ^{146}Gd, which is assumed to be the core nucleus. This treatment is analogous to that applied in Ref. [23] to the ^{211}At nucleus, which, like ^{149}Ho, has three protons outside the closed shell. The positive-parity states likely result from configurations such as $\pi(h_{11/2}^3) \otimes (\pi h_{11/2} \nu d_{5/2}^{-1})_{3^-}$, $\pi(h_{11/2}^3) \otimes (\pi h_{11/2} \nu d_{5/2}^{-1})_{5^-}$, and $\pi(h_{11/2}^3) \otimes (\pi h_{11/2} \nu d_{5/2}^{-1})_{7^-}$.

TABLE VI. Experimental and calculated excitation energies of three-proton levels in ^{149}Ho. Calculations are based on the empirical single-particle (^{147}Gd,^{145}Gd,^{145}Eu,^{147}Tb) and two-proton (^{148}Dy) interaction energies, energies of core-excited states (^{146}Gd), and contributions from interaction energies between proton and neutron particles or neutron holes (^{148}Tb,^{146}Tb). Energies ϵ_J^{calc} are deduced from the relation $\epsilon_J^{calc} = E_J^0 + \Delta_J^k - E_J^g$, where E_J^g is the ground-state energy relative to the ^{146}Gd core, Δ_J^k is the total residual interaction energy of the k states, having the same spin J, and E_J^0 is the zero-order energy, i.e., the sum of single-particle energies of a given configuration.

Main configuration	J^π	E_J^0, 0-order energy	Δ_J^k	$E_J = \Delta_J^k + E_J^0$	ϵ_J^{calc}	ϵ_J^{exp}	$\Delta\epsilon = \epsilon_J^{exp} - \epsilon_J^{calc}$
$\pi(h_{11/2}^3)$	$3/2^-$	3 × (1820) = −5460	−417	−5877	2147		
–	$5/2^-$		−653	−6113	1911		
–	$7/2^-$		−1111	−6571	1426	1415[a]	−11
–	$9/2_1^-$		−1634	−7094	930		
–	$9/2_2^-$		−363	−5823	2201	2209[a]	−8
–	$11/2_1^-$		−2564	−8024	0		
–	$11/2_2^-$		−664	−6124	1900		
–	$13/2^-$		−864	−6324	1700		
–	$15/2_1^-$		−981	−6451	1573	1560	−13
–	$15/2_2^-$		−110	−5570	2454		
–	$17/2^-$		−188	−5648	2376		
–	$19/2^-$		−202	−5662	2362	2285	−77
–	$21/2^-$		+105	−5355	2669		
–	$23/2^-$		+143	−5317	2707	2591	−116
–	$27/2^-$		+290	−5170	2854	2735	−119
$\pi(h_{11/2}^3)(\pi h_{11/2} \nu g_{7/2}^{-1})$	15/2+	−4594	−1746	−6340	1320	1379	+59
–	19/2+	−4594	−1123	−5717	2019	2023	+4
–	23/2+	−4594	−456	−5050	2439	2406	−33
$\pi(h_{11/2}^3)(h_{11/2} d_{5/2}^{-1})_{3-}$	33/2+				3977	3930	−47
$\pi(h_{11/2}^3)(h_{11/2} d_{5/2}^{-1})_{5-}$	37/2+				4483	4329	−154
$\pi(h_{11/2}^3)(h_{11/2} d_{5/2}^{-1})_{7-}$	41/2+				4742	4764	+22
$\pi(h_{11/2})^3(h_{11/2}^2 d_{5/2}^{-2})_{10^+}$	47/2−				6600		

[a]Levels observed in the EC decay of ^{149}Er [22].

These configurations give maximum aligned spins of $J^\pi = 33/2^+$, $37/2^+$, and $41/2^+$, respectively. Possible negative-parity high-spin states could result from the $[\pi(h_{11/2})^3 \otimes (\pi h^2_{11/2}\nu d^{-2}_{5/2})_{10^+}]_{47/2^-}$ configuration. So one may expect a sequence of levels at a still higher excitation energy, $E_x > 4$ MeV. The high-spin core-excited states in ^{149}Ho can be approximated by the leading $\pi(h^3_{11/2})_{27/2^-} \otimes (\pi h_{11/2}\nu d^{-1}_{5/2})_{3^-}$ configuration (e.g., for the $33/2^+$ state). Their excitation energy can consist of three contributions, the proton $\pi(h^3_{11/2})_{27/2^-}$ energy, the core-excited $(h_{11/2}d^{-1}_{5/2})_{3^-}$ energy, and the $h_{11/2}d^{-1}_{5/2}$ interaction energy. The first two terms are obtained from the appropriate excitation energies in ^{149}Ho ($27/2^-$ state) and ^{146}Gd. The last term can be obtained from each of the three protons interacting with the excited particle and hole states of the core. The sum of the three terms gives the estimated energy of the considered states (see Table VI, where the possible candidates for positive-parity core-excited states are listed). According to our guess the calculated $33/2^+$ state at 3977 keV refers to (31/2,33/2), 3930-keV excitation. In a similar way, the $37/2^+$ state at 4483 keV refers to (35/2,37/2), 4329-keV and the $41/2^+$ state at 4742 keV refers to (39/2,41/2), 4764-keV excitation energy. Unfortunately, the negative-parity state with spin 47/2 predicted at an energy of about 6 MeV was not observed.

V. CONCLUSIONS

In the present work we have investigated excited states in ^{148}Ho and ^{149}Ho using in-beam and off-beam spectroscopy methods and (^{40}Ar, $xpyn$) reactions. The lifetime of the known 10^+ isomer in ^{148}Ho was reinvestigated. Spin and parity of 5^- have been assigned to the 9.59-s isomer in ^{148}Ho based on results of the conversion electron measurements. Previously unknown excited states above the 10^+ isomer in ^{148}Ho and above the $27/2^-$ isomer in ^{149}Ho were proposed. The calculated 11^- level in ^{148}Ho has a $\pi(h^3_{11/2})_{27/2}\nu d^{-1}_{5/2}$ configuration. According to our calculations the $12^{(-)}$, $13^{(-)}$, $14^{(-)}$, $15^{(-)}_1$, and $15^{(-)}_3\hbar$ states also have the same configuration (Table V). We observe their counterparts in the experiment (Fig. 6) if the 544.3- or 545.2-keV transition is of an E1 nature. If the 1646-keV state is of positive parity (as the experiment suggests), one can classify it as an 11^+ member of the $\pi h_{11/2}\nu h^{-1}_{11/2}$ configuration.

In ^{149}Ho a few high-spin states have been suggested to be built of valence protons coupled to particle-hole excitations in the ^{146}Gd core. Shell model calculations have been performed for the proposed configurations, supporting this suggestion. It can be concluded that the ^{148}Ho and ^{149}Ho nuclei offer the possibility to test the nuclear shell model regarding general trends and also the details. For a full discussion of the observed high-lying states, more extensive experimental data, especially on states originating from the $\pi(h^3_{11/2})_{27/2} \otimes$ (core) configuration, are required.

ACKNOWLEDGMENTS

We wish to thank the HIL crew for providing excellent beam conditions and for all support at each stage of the work. Special thanks are due to J. Żylicz for very fruitful discussions.

[1] J. Pedersen, B. B. Back, F. M. Bernthal, S. Bjørnholm, J. Borggreen, O. Christensen, G. Folkmann, B. Herskind, T. L. Khoo, M. Neiman, F. Pühlhofer, and G. Sletten, Phys. Rev. Lett. **39**, 990 (1977).

[2] R. Broda, Y. H. Chung, P. J. Daly, Z. W. Grabowski, J. McNeill, R. V. F. Janssens, and D. C. Radford, Z. Phys. A **316**, 125 (1984).

[3] R. Broda, P. J. Daly, J. H. McNeill, Z. W. Grabowski, R. V. F. Janssens, R. D. Lawson, and D. C. Radford, Z. Phys. A **334**, 11 (1989).

[4] T. L. Khoo, R. K. Smither, B. Haas, O. Hausser, H. R. Andrews, D. Horn, and D. Ward, Phys. Rev. Lett. **41**, 1027 (1978).

[5] J. Jastrzębski, R. Kossakowski, J. Łukasik, M. Moszyński, Z. Preibisz, S. André, J. Genevey, A. Gizon, and J. Gizon, Phys. Lett. B **97**, 50 (1980).

[6] J. Wilson, S. R. Faber, P. J. Daly, I. Ahmad, J. Borggreen, P. Chowdhury, T. L. Khoo, R. D. Lawson, R. K. Smither, and J. Blomqvist, Z. Phys. A **296**, 185 (1980).

[7] J. Andrzejewski, A. Król, J. Perkowski, K. Sobczak, R. Wojtkiewicz, M. Kisieliński, J. Kowalczyk, J. Kownacki, and A. Korman, Nucl. Instrum. Methods A **585**, 155 (2008).

[8] T. Kibédi, T. W. Burrows, M. B. Trzhaskovskaya, P. M. Davidson, C. W. Nestar, Nucl. Instrum. Methods A **589**, 202 (2008).

[9] W. D. Fromm, L. Funke, and K. D. Schilling, Phys. Scr. **12**, 91 (1975).

[10] M. V. Klimentovskaya, N. A. Lebedev, and A. A. Sorokin, Yad. Fiz. **12**, 460 (1970); Sov. J. Nucl. Phys. **12**, 251 (1971).

[11] S. Z. Gui, G. Colombo, and E. Nolte, Z. Phys. A **305**, 297 (1982).

[12] A. M. Stefanini, P. Kleinheinz, and M. R. Maier, Phys. Lett. B **62**, 405 (1976).

[13] K. S. Toth, D. C. Sousa, J. M. Nitschke, and P. A. Wilmarth, Phys. Rev. C **37**, 1196 (1988).

[14] E. Nolte, S. Z. Gui, G. Colombo, G. Korschinek, and K. Escola, Z. Phys. A **306**, 223 (1982).

[15] A. Gadea, B. Rubio, J. L. Taín, J. Rico, J. Bea, L. M. García-Raffi, P. Kleinheinz, D. Schardt, E. Roeckl, R. Kirchner, and J. Blomqvist, Z. Phys. A **355**, 253 (1996).

[16] J. L. Taín, B. Rubio, P. Kleinheinz, D. Schardt, R. Barden, and J. Blomqvist, Z. Phys. A **333**, 29 (1989).

[17] V. Rahkonen, I. Bergström, J. Blomqvist, O. Knutilla, K.-G. Rensfelt, J. Sztarkier, and K. Westerberg, Z. Phys. A **284**, 357 (1978).

[18] J. Blomqvist, P. Kleinheinz, and P. J. Daly, Z. Phys. A **312**, 27 (1983).

[19] R. Collatz, N. Amzal, Z. Méliani, C. Schück, Ch. Vieu, J. S. Dionisio, P. Kleinheinz, and J. Blomqvist, Z. Phys. A **359**, 113 (1997).

[20] C. Y. Xie, X. H. Zhou, Y. Zheng, Y. H. Zhang, Z. Liu, Z. G. Gan, T. Hayakawa, M. Oshima, T. Toh, T. Shizuma, J. Katakura, Y. Hatsukawa, M. Matsuda, H. Kusakari, M. Sugawara, K. Furuno, and T. Komatsubara, Eur. Phys. J. A **19**, 7 (2004).

[21] R. D. Lawson, Z. Phys. A **303**, 51 (1981).

[22] R. B. Firestone, J. M. Nitschke, P. A. Wilmarth, K. Vierinen, J. Gilat, K. S. Toth, and Y. A. Akovali, Phys. Rev. C **39**, 219 (1989).

[23] I. Bergström, J. Blomqvist, P. Carlé, B. Fant, A. Källberg, L. O. Norlin, K.-G. Rensfelt, and U. Rosengaard, Phys. Scr. **31**, 333 (1985).